

Hole-Assisted Energy Deposition in Clusters and Dielectrics in Multiphoton Regime

G. L. Yudin¹, L. N. Gaier², M. Lein³, P. L. Knight²,
P. B. Corkum¹, and M. Yu. Ivanov¹

¹ Femtosecond Science Program, Steacie Institute for Molecular Sciences, National Research Council of Canada,
100 Sussex Drive, Ottawa, K1A 0R6 Canada

e-mail: gennady.yudin@nrc.ca

² Blackett Laboratory, Imperial College of Science, Technology and Medicine, London, SW7 2BW United Kingdom

e-mail: lucien.gaier@ic.ac.uk

³ Max Planck Institute for the Physics of Complex Systems, Nöthnitzer Strasse 38, D-01187 Dresden, Germany

Received February 5, 2003

Abstract—A novel mechanism of hole-assisted energy absorption by dielectric materials interacting with ultrashort laser pulses of moderate intensity (below damage threshold) is proposed. The analytical theory of multiphoton absorption is generalized to the cases of hole-assisted processes in laser fields of arbitrary polarization. Numerical simulations of the non-stationary Schrödinger equation in one-dimensional model systems are performed to gauge the validity of the analytical theory. Large (up to several orders of magnitude) enhancements of the multiphoton transition rates are found both numerically and analytically. The applicability of the analytical theory is confirmed up to relatively high Keldysh parameters. We also describe a second novel mechanism of energy absorption: laser-assisted electron avalanche in dielectric materials. Unlike the traditional avalanche, in this process, collisional excitation of new electrons to the conduction band occurs without heating the already free electrons to energies above the bandgap energy. This process should dominate for ultra-short laser pulses which do not give enough time for the development of the traditional avalanche.

1. INTRODUCTION

Traditionally, the dynamics of laser-induced breakdown is divided into three stages (see, e.g., [1–3]). At the first stage, conventional multiphoton ionization provides seed population of free electrons. At the second stage, these electrons increase their kinetic energy due to inverse bremsstrahlung in the laser field, as a result of multiple laser-assisted collisions with lattice. This “heating” stage is accompanied by electron loss due to recombination and diffusion. The third stage starts when the electron energy exceeds the bandgap, so that the electron can collisionally promote a next electron into the conduction band.

Typically, efficient collisional excitation requires that the electron energy exceed the bandgap by a factor of about two (i.e., at the maximum of the inelastic collision cross section). It is often assumed that the breakdown occurs when the electron density exceeds a threshold value, typically $n_{\text{th}} \sim 10^{18} \text{ cm}^{-3}$. The development of the avalanche due to free-electron heating in electron–phonon–photon collisions in competition with relaxation through electron–electron and electron–phonon collisions is a relatively slow process, which usually takes a few tens of femtoseconds [3]. A recent experimental and theoretical study of bulk damage in fused silica [4] induced by intense infrared laser pulses supports this picture. The physics of energy deposition should inevitably change when extremely short low-frequency fs laser pulses (only a few cycles long)

interact with transparent dielectric materials. As a simple estimate, let us assume that the laser wavelength is 800 nm, the pulse duration is about 10 fs or even less, and that the material is fused silica with a bandgap of 9 eV. Experimentally, the typical intensities resulting in permanent modification of dielectrics are $I \sim 10^{13} \text{ W/cm}^2$. The characteristic electron oscillation energy is $U_p = e^2 E^2 / 4m\omega^2$, where ω is the laser frequency and E is the electric field strength. At $I = 10^{13} \text{ W/cm}^2$ and $\lambda = 800 \text{ nm}$, we have $U_p = 0.6 \text{ eV}$.

When the electron is promoted to the conduction band and oscillates in the laser field, on average it absorbs an energy $\Delta E \sim 2U_p$ per collision provided they do not occur more frequently than once per laser half-cycle. Assuming that the multiphoton transition of the seed electrons to the conduction band occurs near the peak of the 10 fs pulse and completely neglecting any energy loss, we see that in the following 5 fs (2 cycles) the electron would absorb at most 4–5 eV, i.e., less than the bandgap energy. Absorbing 10–20 eV in such optimal conditions of well-timed collisions and negligible energy loss would require about 15–25 fs, which would correspond to pulse durations of 30–50 fs. This is roughly the typical pulse duration at which the traditional avalanche starts to dominate.

We show that under these conditions there are two new physical mechanisms which lead to accelerated ionization and require either no or minimal heating of the electrons in the conduction band. The same physics

applies to multiple ionization of clusters and molecules. One of the physical mechanisms described below for dielectrics is analogous to *enhanced ionization* of molecules [5] and is known as *ionization ignition* in clusters [6]. For clusters, it has been studied in the high-intensity regime of Coulomb explosion and formation of multiply charged atomic ions [7]. Here, we restrict our consideration to the moderate intensity regime and provide its analytical description.

2. PHYSICS AND STAGES OF ENHANCED ENERGY ABSORPTION IN SHORT PULSES

The first stage in energy absorption is multiphoton ionization (MPI), which seeds the electron density in the conduction band of a dielectric material and/or creates free electrons and ions in a cluster. The energy absorption rate at this stage has been already described by L.V. Keldysh [8] and has been consistently used ever since (see, e.g., [4]).

The key quantitative flaw of the rate [8] is that it ignores possible exponential enhancement of the multiphoton absorption rate due to already present positive and negative charges: holes and electrons in the conduction band of a dielectric (or in the cluster). We now describe the physics of such enhancement.

2.1. Cold Electron-Hole-Assisted MPI

Immediately following MPI, an electron–hole pair can change the rates of multiphoton absorption by adjacent atoms (molecules, lattice sites) due to the electric fields created by the electron and ion (hole). Consider the example of a noble gas cluster with typical inter-atom distances $D \sim 6\text{--}8$ a.u. The less mobile ion (hole) creates a dc electric field acting on adjacent atoms. The much lighter electron driven by the laser field does not leave the vicinity of the parent ion immediately and, while it has not been substantially accelerated, also provides a slowly changing electric field. As in enhanced ionization of molecules, both fields act together with the laser field on the adjacent atoms to modify the barrier for ionization. This combined action of both charged particles ends when the light electron leaves the vicinity of the parent ion, not only due to drift but also due to fast spreading of the wavepacket. The latter can be estimated using the uncertainty in the electron velocity after ionization [9] $\Delta v \sim \sqrt{E/\sqrt{2I_p}}$, where E is the strength of the laser field and I_p is the ionization potential. Simple estimate shows that, in about one half of the laser cycle, the spreading alone separates the electron and parent ion by an additional distance of $2D - 3D$ for intensities $I \sim 10^{13}$ W/cm².

For much high laser intensities, typical for Coulomb explosions of clusters, the electron is driven away from the vicinity of the parent ion and out of the cluster much faster.

Large spatial separation of the electron and ion (hole) completes the first stage. Most of the time, the electron and the ion (hole) are well separated spatially and their effects can be considered separately.

2.2. Collision-Assisted Multiphoton Avalanche

The first effect is collision-assisted multiphoton excitation of valence electrons from the valence band to the conduction band. This process uses energy both from the laser photons and from an electron in the conduction band with the kinetic energy $\mathcal{E}_K < I_p$, where I_p is the bandgap energy. During collision, the free electron in the conduction band transfers energy $\Delta\mathcal{E}$ to the electron in the valence band, resulting in virtual excitation of the latter. The rest of the energy needed for a real transition to the conduction band is supplied by the strong laser field. For example, if the electron has energy $\mathcal{E}_K = 4$ eV $< I_p$, it can help the laser field to promote the next electron to the conduction band by giving up to 4 eV of its energy to that electron. In the absence of the laser field, this would be an elastic collision.

Just as in traditional avalanche, the probability of this process is proportional to the concentration of free electrons in the conduction band. Below, we will show that, as compared to direct multiphoton excitation, collision-assisted excitation provides exponential enhancement of the transition rate.

The detailed theory of this process will be described elsewhere.

2.3. Hole-Assisted Multiphoton Absorption

The second effect which leads to exponential enhancement of the multiphoton absorption rate is related to the presence of ions (holes). This mechanism is similar to enhanced ionization of molecules [5] and ionization ignition in clusters [6, 7], but the intensities considered here are significantly lower.

Atoms or molecules adjacent to the ion (hole) feel the combination of the oscillating laser field $\mathbf{E}(t) = \mathbf{E}_0 \cos \omega t$ and the constant electric field of the hole: $\mathbf{E}_h = \mathbf{R}/R^3$, where \mathbf{R} is the radius vector to the hole. Extra electric field results in exponential enhancement of the transition rate. For example, if multiphoton ionization occurs in the tunneling regime of $\gamma^2 = I_p/2U_p \ll 1$, the quasistatic tunneling rate

$$\Gamma_{qs}(t) \propto \exp\left(-\frac{2(2I_p)^{3/2}}{3|\mathbf{E} \cos \omega t|}\right) \quad (1)$$

is modified by adding the static field of the positive charge, $|\mathbf{E} \cos \omega t| \rightarrow |\mathbf{E} \cos \omega t + \mathbf{E}_h|$. This limit has been studied in [5–7].

Thus, the creation of an ion (hole) exponentially enhances the creation of new ions (holes) at adjacent lattice sites. As soon as the new ions (holes) are created, they continue the same trend. The propagation of this

ionization is similar to that of forest fires. At relatively low densities, each ion (hole) serves as a nucleation site around which new ions (holes) are created. As the ionized region grows, the role of the original ions (holes) left in the middle diminishes. The expansion of the region continues along its perimeter (surface). The forest fire process will be described elsewhere.

Both effects described above behave in an avalanche-like manner. Both yield exponential enhancement of the multiphoton transition rate. Both do not require substantial heating of the electrons. The first effect exists for any energy of the free electrons but is important when this energy is substantial (e.g., exceeds the photon energy and is a significant fraction of the bandgap). The second mechanism does not use any kinetic energy of the electrons at all. Both include multiphoton absorption as part of the transition and are inherently weak as compared to standard collisional excitation of electrons across the bandgap. However, short pulses do not give sufficient time to the conventional heating of the electrons. Traditional avalanche does not develop, and the new mechanisms should become dominant.

3. THEORY OF HOLE-ASSISTED ABSORPTION AT MODERATE INTENSITIES

3.1. Analytical Model

Let us start by looking at the linearly polarized field $\mathbf{E} \cos \omega t$. The electric field of the hole is \mathbf{E}_h . The total electric field acting upon an atom at the lattice site is

$$\mathbf{E}_{\text{tot}}(t) = \mathbf{E} \cos \omega t + \mathbf{E}_h, \quad (2)$$

and the corresponding vector potential is

$$\mathbf{A}_{\text{tot}}(t) = -\frac{\mathbf{E}}{\omega} \sin \omega t - \mathbf{E}_h t. \quad (3)$$

The population of continuum states at instant t is

$$W(t) = \int d^3 \mathbf{v} |a_{\mathbf{v}}(t)|^2, \quad (4)$$

where $a_{\mathbf{v}}(t)$ is the probability amplitude of populating the field-free continuum state labeled by the velocity $|\mathbf{v}\rangle$.

Using the strong-field approximation, we can write

$$a_{\mathbf{v}}(t) \sim -i \int_{-\infty}^t dt' V_{vc}(t') \exp(-iS_{\mathbf{v}}(t, t')), \quad (5)$$

where V_{vc} is the transition dipole matrix element between the valence and the conduction bands induced by the total field, $V_{vc}(t') \propto \mathbf{r}_{vc} \cdot \mathbf{E}_{\text{tot}}(t')$, and

$$S_{\mathbf{v}}(t, t') = I_p(t-t') + \frac{1}{2} \int_{t'}^t dt'' [\mathbf{v} - \mathbf{A}_{\text{tot}}(t) + \mathbf{A}_{\text{tot}}(t'')]^2 \quad (6)$$

is the action integral.

The integral over t' for the amplitude $a_{\mathbf{v}}(t)$ can be calculated using the saddle point method. The saddle points $t'(t)$ are given by the equation

$$\frac{1}{2} [\mathbf{v} - \mathbf{A}_{\text{tot}}(t) + \mathbf{A}_{\text{tot}}(t')]^2 + I_p = 0. \quad (7)$$

Due to the periodicity of the laser field, for any moment of observation t there are many saddle points t'_n separated by a laser cycle. They correspond to contributions to the total amplitude from repeated ionization events for each laser cycle. For the saddle point closest to t , denoted as t'_0 , $\text{Re}(t'_0) \approx t$. Other t'_n are separated from t'_0 by the integer number of cycles, $t'_n = t'_0 - 2\pi n$, where integer $n \geq 1$. The imaginary part of action is the same for all of them,

$$\text{Im}[S_{\mathbf{v}}(t, t'_n)] = \text{Im}[S_{\mathbf{v}}(t, t'_0)], \quad (8)$$

and hence they all yield the same exponential dependence for the ionization probability.

To calculate the latest addition to the continuum population, we select only a single saddle point t'_0 with $\text{Re}(t'_0) \approx t$. Contributions from the saddle points t'_n , with $n \geq 1$, describe the population created in the continuum one or more laser cycles ago; the corresponding action integrals contain contributions from the free electron motion in the continuum.

To calculate the main exponential dependence of the ionization rate on the total field, we can follow the prescription from [10]. The method does not give the correct pre-exponential factor but allows one to obtain the exponent in a simple and painless way. The key point is that if the electron has just shown up in the continuum at t , its velocity \mathbf{v} is small. In other words, one drops \mathbf{v} from the saddle point equation, which then becomes

$$\frac{1}{2} [\mathbf{A}_{\text{tot}}(t'_0) - \mathbf{A}_{\text{tot}}(t)]^2 + I_p = 0. \quad (9)$$

Now, for simplicity, we assume that the field of the hole is parallel to the laser polarization. One can do other orientations just as easily. Then, introducing the notation $\phi = \omega t$, $\omega t'_0 = \omega t - \theta = \phi - \theta$, the saddle point equation becomes

$$\sin(\phi - \theta) + \mu(\phi - \theta) = -i\gamma + \sin \phi + \mu\phi, \quad (10)$$

where $\mu = E_h/E$ and γ is the Keldysh parameter.

Unfortunately, this equation cannot be solved analytically. However, its numerical solution is trivial. Once it is found, the exponential dependence in the transition amplitude $a_{\mathbf{v}=0}(t)$ is given by the imaginary part of the corresponding action integral and the rate is proportional to that exponent squared:

$$\Gamma = N \exp(-2\text{Im} S_{\mathbf{v}=0}(t, t'_0)). \quad (11)$$

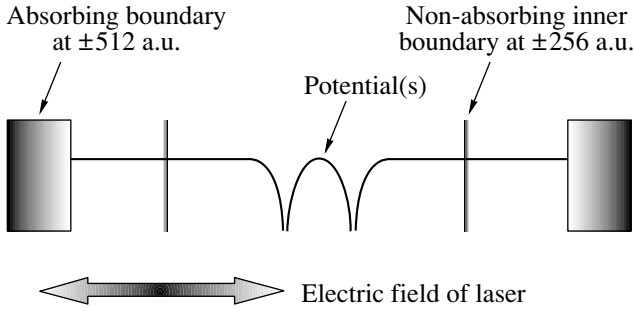


Fig. 1. One-dimensional model grid used to represent the SiO_2 well and positive potential separated by a distance D .

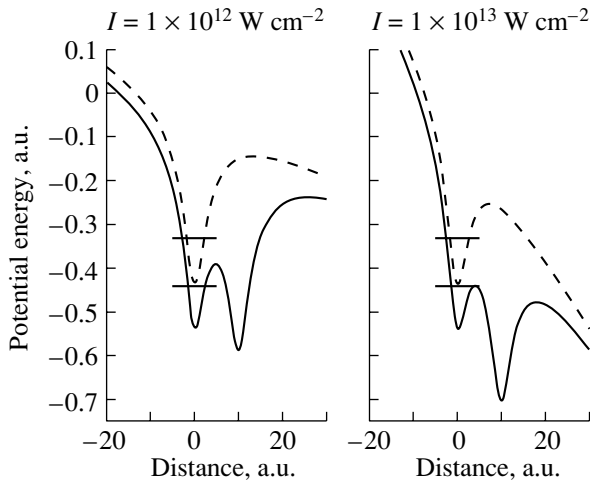


Fig. 2. Atomic potentials with (solid line) and without (dashed line) the hole ($D = 10$ a.u.) using a full-potential description for $I = 10^{12}$ W/cm^2 and $I = 10^{13}$ W/cm^2 . Ground-state energies are shown by bars.

The pre-exponential factor N can be written following [10]. For our case of $\gamma \sim 1$, this factor can (and should) be calculated for the peak of the instantaneous electric field and is given in [10].

3.2. Numerical Simulations

To gauge the validity of the above analytical model, we have performed numerical simulations using a one-dimensional grid 1024 a.u. in size (4096 grid points separated by 0.25 a.u.) with a soft-core potential well located at its center (considered to be $x = 0$). Within this first well sits the ground-state wavepacket of an electron. The ground-state energy of 9 eV for SiO_2 is reproduced using a soft-core parameter $\epsilon = 5.2$ (in atomic units) in a regularized potential:

$$V = -\frac{1}{\sqrt{x^2 + \epsilon}}. \quad (12)$$

The determination of the ground state and the propagation of the wavefunction is accomplished using the split-operator method and is carried out within the length gauge. The absorbing boundary region of the grid is set to be 1/8 the total grid size, with a \sin^2 mask function within the boundary region. A non-absorbing boundary called the “inner” boundary is placed at ± 256 a.u. from the core (see Fig. 1). It is used to compute norm values and ionization rates far from the absorbing boundaries and as such can be considered unaffected by the absorbing mask function.

The significance of the inner boundary can be seen in the results: the norms and ionization rate values taken at both boundaries are qualitatively the same for almost any intensity. Quantitatively, there is little difference except that the rates calculated at the inner boundary are slightly higher than those calculated at the absorbing boundary. This is simply due to the increased time it takes the wavepacket to reach the outer boundary, during which additional packet spreading occurs.

The addition of one positive potential hole has so far been attempted. It is a soft core potential well, identical to the first, located at a distance D . The hole is either suddenly switched on at the beginning of the laser pulse or linearly switched on during the on-ramp of the laser pulse. Figure 2 shows the combined potentials of the “with hole” and “without hole” systems, as given by Eq. (13) (the “full-potential” (FP) description used numerically):

$$V = -\frac{1}{\sqrt{x^2 + \epsilon}} - \frac{1}{\sqrt{(x-D)^2 + \epsilon}}. \quad (13)$$

As discussed earlier, the analytic theory assumes the combined system potential to be given by

$$V = -\frac{1}{\sqrt{x^2 + \epsilon}} - \frac{x}{D^2}. \quad (14)$$

Using this approximation rather than the FP description used in the simulations will be shown later to give significantly different ionization enhancement behaviors. The differing geometrical situation can be seen by comparing Fig. 2 with Fig. 3. This will be discussed further in the next section.

Laser intensities used in the theory and numerics typically range from $I \sim 10^{11}$ W/cm^2 to $I \sim 10^{14}$ W/cm^2 , with a laser wavelength of 800 nm. The most interesting region lies within the range $I \sim 10^{12}$ W/cm^2 to $I \sim 10^{13}$ W/cm^2 for SiO_2 , as it is the region for which the electric fields of the hole and the laser pulse become comparable. Furthermore, it can be seen in Fig. 2 that, at $I = 10^{13}$ W/cm^2 and above, barrier suppression is observed in the potential from which the electron wavepacket is born (and, hence, tunneling solutions are no longer applicable). The pulse shape is generally trapezoidal, with linear ramping on and off of two laser

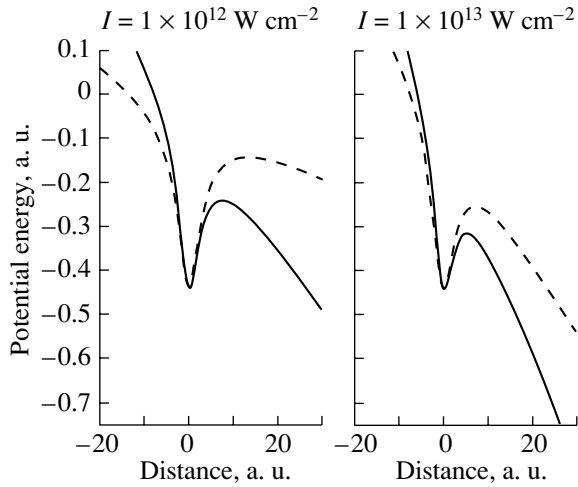


Fig. 3. Atomic potentials with (solid line) and without (dashed line) the hole ($D = 10$ a.u.) using the homogeneous dc-field description for $I = 10^{12}$ W/cm² and $I = 10^{13}$ W/cm².

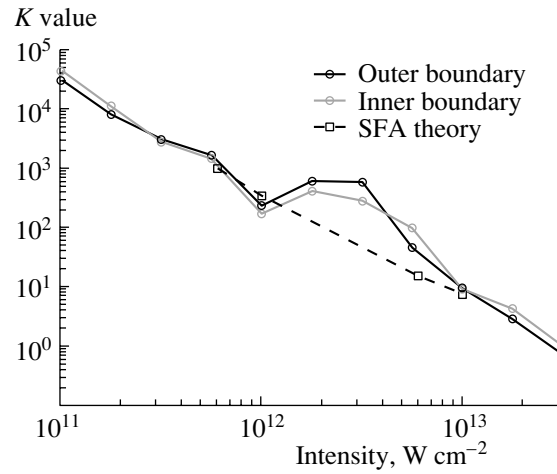


Fig. 4. Enhancement values plotted against intensity for $D = 10$ a.u. with a sudden turn-on of the hole. The laser pulse was of the 2-6-2 form at a wavelength of 800 nm.

cycles and with the range of 6 laser cycles at maximum intensity being used in the results so far.

4. RESULTS AND DISCUSSION

To quantify the effect that the proximity of the hole has, the enhancement factor K in the ionization rates Γ is calculated. SFA analytic values are denoted by K_a , whereas numerical enhancement values (K_n) are calculated as the ratio of the ionization rates with a hole (Γ_1) against rates without a hole (Γ_0):

$$K_n = \frac{\Gamma_1}{\Gamma_0}. \quad (15)$$

The rates Γ_0 and Γ_1 are calculated as the rate of change of the total norm of the wavepacket at the absorbing boundaries (not the inner boundaries). The time-dependent norms produced by the code are then fitted to an exponential rate equation,

$$|\psi(t)|^2 = |\psi(t_0)|^2 e^{-\Gamma(t-t_0)}, \quad (16)$$

using a χ^2 minimizing technique. This technique involves maximizing the “goodness-of-fit” of the merit function χ^2 relating the rate equation to the numerical data.

Figure 4 shows the results for the case of SiO₂ and a short 2-6-2 trapezoidal laser pulse. The ion is suddenly turned on at the beginning of the laser pulse in both cases (that is, the second potential is born as the laser pulse begins ramping). This has important consequences for the subsequent behavior of the electron, as its initial lowest energy state is changed suddenly from a single potential system to a dual potential system (in the full-potential description). This encourages ionization of parts of the wavepacket, even without the influence of the laser field, although the proportion ionized

is small. The effect of using a more gentle turn-on of the nearby ion is discussed later for the case of an Ar cluster.

In the analytic theory, as D increases, K_a falls, whereas in the numerics this is not so obvious: K_n values remain roughly constant with D . This is due to the different geometries employed by theory and numerics when describing the ion. The homogeneous dc field description of the hole ignores the evolution of the wavepacket when it is on the side of the well away from the ion. The FP description used in the numerical simulations seems to lead to resonance type behavior at certain intensities. The laser induces Stark shifts in the energy levels of the system, and thus a variation in

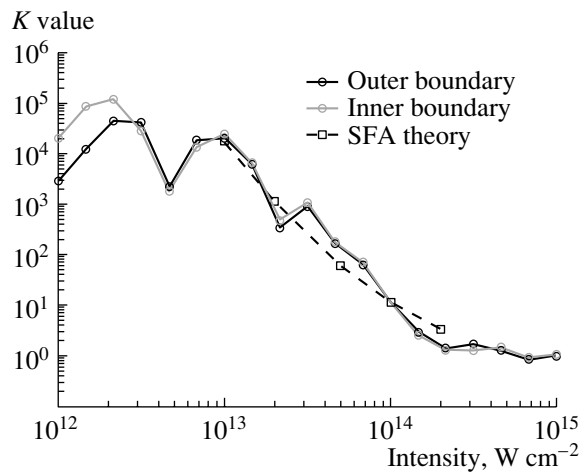


Fig. 5. Argon enhancement values plotted against intensity for $D = 7$ a.u. with a sudden turn-on of the hole. The laser pulse was of the 2-6-2 form at a wavelength of 800 nm.

intensity may bring certain transitions in and out of resonance. This leads to the “knee” and “peak” features in the enhancement profiles.

Consider now the corresponding results for the Ar clusters. Both analytical and numerical results can be seen in Fig. 5. There appears to be fairly strong agreement between theory and numerics in the tested intensity range, although there are large dips in the enhancement curves at two points. This appears not to be due to the absorbing boundary (as the inner boundary calculations follow the same trend). This can be explained by a resonance-type effect due to the differing geometries of the atom–hole systems in theory and numerics. The SFA theory does not take the nature of the birth of the ion site into account, which, according to the numerical calculations, is important at intensities less than $I \sim 10^{12}$ W/cm².

5. CONCLUSIONS

Comparison between analytical and numerical results shows that the enhancement coefficients can be estimated using SFA up to unexpectedly high values of $\gamma \sim 4$. The analytical theory allows one to easily consider cases of arbitrary polarization. The theory shows that circular polarization is preferable for obtaining large enhancement coefficients. Indeed, for linear polarization, the best geometry corresponds to the case when the direction to the ion (hole) is parallel to the electric field. For circular polarization, this does not matter, so long as the direction to the ion (hole) is in the plane of laser polarization. For example, for an Ar cluster, when the linear polarization is perpendicular to the atom–ion axis, the enhancement is 35 times less than for the same strength of the circular field at $I = 5 \times 10^{13}$ W/cm² and $D = 6$ a.u.

In conclusion, two novel mechanisms (hole-assisted energy absorption and laser-assisted electron avalanche) for energy deposition in dielectrics interacting with ultra-short laser pulses have been suggested. Detailed comparison between numerical and analytical results for hole-assisted energy absorption confirmed the analytical model and established its accuracy and validity regimes. The generalized SFA theory was

developed for laser fields with linear and circular polarizations and any geometry of holes.

ACKNOWLEDGMENTS

This work was supported by the EPSRC and the NRC-BC grant 00CRP13. LNG would like to thank Pier-Paolo Corso (University of Palermo, Sicily) for his invaluable help in testing and improving the numerical code.

REFERENCES

1. M. Sparks *et al.*, Phys. Rev. B **24**, 3519 (1981); M. V. Fischetti *et al.*, Phys. Rev. B **31**, 8124 (1985); B. C. Stuart *et al.*, Phys. Rev. Lett. **74**, 2248 (1995); Phys. Rev. B **53**, 1749 (1996); T. Apostolova and Y. Hahn, J. Appl. Phys. **88**, 1024 (2000).
2. D. Du *et al.*, Appl. Phys. Lett. **64**, 3071 (1994); P. P. Pronko *et al.*, Phys. Rev. B **58**, 2387 (1998); M. Lenzner *et al.*, Phys. Rev. Lett. **80**, 4076 (1998); A.-C. Tien *et al.*, Phys. Rev. Lett. **82**, 3883 (1999).
3. A. Kaiser *et al.*, Phys. Rev. B **61**, 11 437 (2000).
4. L. Sudrie *et al.*, Phys. Rev. Lett. **89**, 186 601 (2002).
5. T. Seideman, M. Yu. Ivanov, and P. B. Corkum, Phys. Rev. Lett. **75**, 2819 (1995); Chem. Phys. Lett. **252**, 181 (1996); S. Chelkowski and A. D. Bandrauk, J. Phys. B **28**, L723 (1995); M. Ivanov *et al.*, Phys. Rev. A **54**, 1541 (1996); G. N. Gibson, G. Dunne, and K. J. Bergquist, Phys. Rev. Lett. **81**, 2663 (1998).
6. C. Rose-Petruck *et al.*, Phys. Rev. A **55**, 1182 (1997); S. X. Hu and Z. Z. Xu, Phys. Rev. A **56**, 3916 (1997).
7. V. Veniard, R. Taieb, and A. Maquet, Phys. Rev. A **60**, 3952 (1999); Phys. Rev. A **65**, 013202 (2001); I. Last and J. Jortner, Phys. Rev. A **62**, 013201 (2000); C. Siedschlag and J. M. Rost, Phys. Rev. Lett. **89**, 173401 (2002).
8. L. V. Keldysh, Zh. Éksp. Teor. Fiz. **47**, 1945 (1964) [Sov. Phys. JETP **20**, 1307 (1965)].
9. See, e.g., N. B. Delone and V. P. Krainov, *Multiphoton Processes in Atoms* (Springer, Berlin, 1994); G. L. Yudin and M. Yu. Ivanov, Phys. Rev. A **63**, 033404 (2001); Phys. Rev. A **64**, 019902(E) (2001); Phys. Rev. A **64**, 035401 (2001).
10. G. L. Yudin and M. Yu. Ivanov, Phys. Rev. A **64**, 013409 (2001).